Opacity measurements of a hot iron plasma using an X-ray laser

M. H. Edwards, D. Whittaker, P. Mistry, N. Booth, G. J. Pert and G. J. Tallents
Department of Physics, University of York, York, YO10 5DD, UK

B. Rus, T. Mocek and M. Kozlová
Department of X-ray Lasers, PALS Research Centre, Institute of Physics, Academy of Sciences of the Czech Republic, 182 21 Prague 8, Czech Republic

C. McKenna, A. Delserieys and C. L. S. Lewis
School of Mathematics and Physics, The Queen's University of Belfast, Belfast, BT7 1NN, UK

M. Notley and D. Neely
Central Laser Facility, CCLRC Rutherford Appleton Laboratory, Chilton, Didcot, Oxfordshire, OX11 0QX, UK

Main contact email address mhe101@york.ac.uk

Introduction

At high temperatures (> 1 eV) where materials are in the plasma state, there have been some measurements of opacity in the EUV (photon energy 10 - 200 eV)[1-3]. However, it has not been possible to make direct opacity measurements of near solid density materials at temperatures > 30 eV because background emission from the material overwhelms the emission from the back-lighter used as the source of radiation for the measurement. Some indirect measurements of opacity at high photon energies (~ 1 keV) and high temperatures (> 50 eV) have been successfully undertaken[4]. The emissivity of thin layers of solid material heated by short laser pulses has been measured and assuming local thermodynamic equilibrium (LTE), the opacity deduced using Kirchhoff's law.

Opacities are important in radiation diffusion models of the sun and other stars[5]. Opacity is also important in indirect drive laser fusion and in materials testing[6]. In indirect drive fusion and the materials testing programs, black-body cavities or hohlraums are created with the energy supplied by large lasers irradiating the cavities walls to produce EUV and X-ray radiation. The radiation temperatures are typically 10 - 200 eV depending on the size of the hohlraum and the laser energy available, so the opacities of materials for 5 - 600 eV photon energy range are important. A new application of opacity measurements will arise with the development of EUV fourth generation light sources based on free-electron lasers[7]. Most of the experiments that will be undertaken when these light sources are built will involve the beams penetrating material. Due to the high intensities, the material will rapidly heat and ionise and it will be important to know the opacity under a wide range of conditions[8].

Experiment

In an experiment using the VULCAN Nd:glass laser at the Rutherford Appleton Laboratory an X-ray laser was generated at 13.9 nm from a 4d-4p transition in nickel-like silver. To obtain a saturated output so that shot-to-shot variations were reduced two 18 mm long silver slabs were aligned 500 microns apart parallel to their surfaces and 150 microns apart perpendicular to their surfaces and each irradiated by three beams of energy ~40 Joules, focussed to a line of 22 mm length by 100 microns width. Irradiance on the targets by each of the six beams was ~2.5×10^{12} Wcm^{-2} in the pre-pulse and ~2.5×10^{13} Wcm^{-2} in the 80 ps main pulse 2.2 ns later. The double pulse technique minimises refraction of the X-ray laser beam, optimises the gain volume and maximises the absorption of the pumping laser beam[9].

A Mo-Si multi-layer mirror imaged the X-ray laser output and focussed it to a spot of diameter ~200 μm onto a sample target to measure its opacity. A second spherical multi-layer mirror imaged the transmitted X-ray laser light onto a back-thinned Andor CCD camera, located ~7 metres away. Baffling prevented unwanted light reaching the detector which was filtered with aluminium and parylene-N, each between 100 and 300 nm thick. The relatively narrow band-width of the multi-layer mirrors (~0.8 nm) also helped to remove unwanted light from reaching the detector. A cross-wire of diameter 100 μm diameter was placed in front of the CCD detector and is clearly visible in the images obtained (see figure 1).

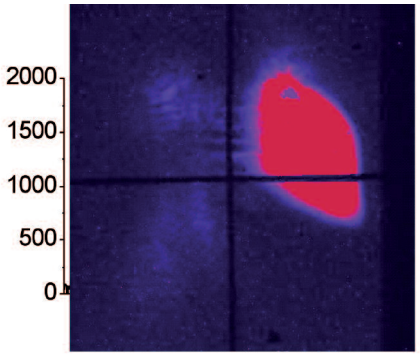

Figure 1. The footprint of the X-ray laser as it passes through the opacity target at a time of 100 ps after the peak of the sample target irradiation. The brighter zone corresponds to the region where the target has been heated and a plasma produced, whilst the most intense component of the X-ray laser beam can be seen towards the left of the image passing through the unheated material. The central region of the heated region (as indicated by the intersection of the arrows) has been used to deduce the transmission of the heated target by comparison to transmission through unheated regions on the same shot.

The sample targets comprised a 50 (± 5) nm iron layer deposited on a 0.53 (± 0.05) micron parylene-N (CH) substrate foil and buried beneath an 80 (± 10) nm layer of parylene-N. The target normal was orientated at 45° to the X-ray laser probe beam. Another ~ 6 - 9 J pulse of 80 ps duration from the VULCAN laser was focussed to a spot of diameter 100 microns at 45° incidence on the

sample target in order to heat the iron layer. The sample targets were designed so that energy from the heating beam would be absorbed into the outer plastic layer, conductively heating the buried iron. This tamping slows down the rate of expansion of the iron layer to provide a plasma of improved uniformity and higher density. Radiative preheating of the buried layer can be ignored as the plastic top layer, once heated, is a weak emitter. Hot electron pre-heating at the employed irradiances (~10^{15} Wcm^{-2}) is also small.

The opacity of the heated and high density iron was determined by measuring the transmission of the X-ray laser beam through the sample target. Having verified the alignment of the X-ray laser through the sample target position to the CCD detector, the self-emission of the plasma produced by heating the sample target was investigated. Compared with the brightness of the X-ray laser probe, the self-emission was found to be negligible at ~100 counts compared with the peak transmission (~10000 counts) at the level of filtering used. The arrival of the sample target heating beam was adjusted to enable probing of the plasma at different times in its evolution.

Results

Figure 1 shows an example footprint of the X-ray laser as it passes through the heated opacity target. The characteristic crescent shape[9] of the most intense part of the X-ray laser beam is visible just to the left of the vertical cross-wire. A weaker, but more uniform part of the diverging X-ray laser beam is transmitted strongly through the heated section and weakly through the surrounding area of the sample target. This lower intensity, but more uniform component of the X-ray laser beam has been used to make measurements of the transmission of the heated iron region by comparing the intensity of the X-ray laser recorded in the heated section of the target with the intensity recorded on the same shot in the unheated section after allowance for the cold iron transmission (see figure 2). The error bars in the experimental points of figure 2 at 100 - 300 ps arise due to the uncertainty in the incident X-ray laser intensity estimated for this procedure. The transmission is approximately constant towards the centre of the heated target, being within ±10% over the heated target area, (see the cross-sections on figure 1) and the transmission measurements of figure 2 are from the central position.

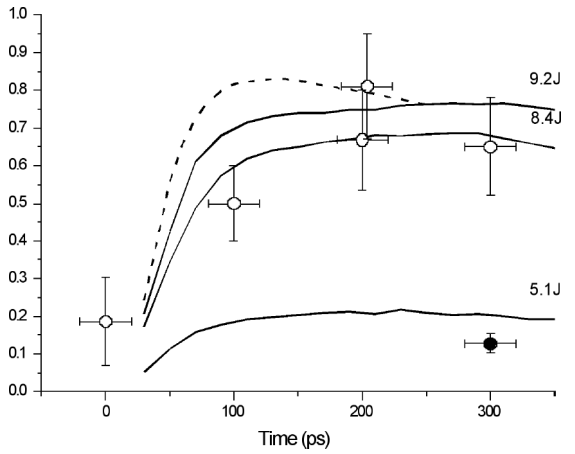

Figure 2. The variation of transmission of a 13.9 nm X-ray laser with time from the peak of the heating pulse through the iron component of the sample target at 45° incidence is shown for both experimental (data points) and simulated data (continuous curves). Experimental data with pulse energies in the range 7 - 9 J are shown as open circles, while a data point with pulse energy 6 J is shown as a filled in circle. Simulations are shown for heating laser energy of 6.5 J using the TOPS data (broken curve) and 9.2 J, 8.4 J and 5.1J using our developed code (as labeled). A measurement of transmission through an unheated target is shown as a data point at time 0 ps.

We have made a measurement of the transmission of the unheated iron component of the targets by comparing the X-ray laser transmission on different shots through the unheated sample target and through a filter of known transmission. This transmission measurement (0.19) is plotted on figure 2 at time zero. The tabulated[10] cold transmission of 50 (±5) nm of iron at 45° incidence is just 0.03 (±0.01) suggesting that the error in the cold iron transmission measurement is large. However, the measurement error is smaller (estimated to be (±20%) for the heated target measurements as they can be obtained in a single shot.

The deduced experimental transmission through the iron layer at 45° incidence is plotted with simulation results obtained using the Ehybrid code and a post processor as outlined in Edwards *et al.*[15] superimposed in figure 2. The outer layer of plastic (80 nm thick) has been ignored in the analysis of the experimental transmission through the iron as its opacity contribution is low due to its untamped expansion (transmission = 0.7 for solid[10] and close to unity once a hot plasma is formed). The transmission of the plastic substrate (0.53 μm thick) has been taken as its solid value throughout (transmission = 0.08) for the deduction of the experimental transmission through the iron. According to our calculations only a small outer fraction (<0.1 μm) of the substrate is ablated during the experiment and even this small fraction is only heated to a few electron-volts and so has a similar opacity to cold plastic.

The horizontal axis of figure 2 measures the delay between the peak of the heating pulse and the peak of the ≈ 40 ps

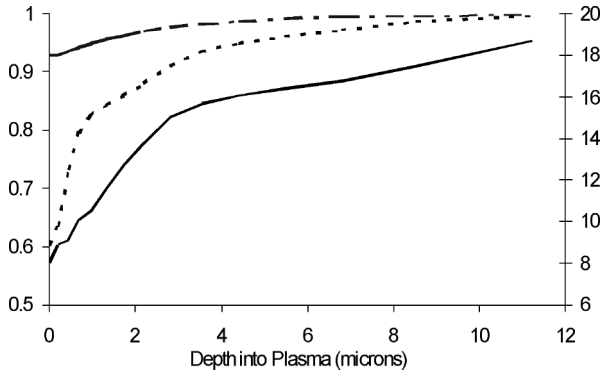

Figure 3. The calculated transmission of 13.9 nm soft X-ray radiation through the iron layer at time 100 ps at 45° incidence as simulated using the EHYBRID fluid code (assuming a pulse energy of 8.4 J) and our model of opacity with (dots) and without (dot-dash) the opacity effect of a large number of bound-bound transitions. The EHYBRID code evaluation of the average degree of plasma ionisation is also shown (solid line).

duration X-ray laser pulse arriving at the opacity target. The experimental data points were obtained with laser pulses pumping the X-ray laser target in the range 30 J to 44 J, though because the X-ray laser was saturated, the measured range of energies in the output X-ray laser pulses was within ±50% of the mean. A range of laser energies irradiated the sample target (6 - 9 J) and this caused some of the range of transmissions seen for the X-ray laser in figure 2. Good agreement can be seen between the experimental data points and modelling data at times of 100 and 200 ps with experimental pulse energies in the range 7 - 9 J. One of the measured transmissions at 300 ps is much lower than that predicted by the simulation with higher laser energies, but is in close agreement with our simulation at the reduced laser energy (5.1 J) corresponding to an energy close to that of the 300 ps data point.

Conclusion

In conclusion, we have demonstrated that an X-ray laser can be used to measure the opacity of hot, dense plasma. The opacity of the expanding plasma reduces rapidly within the first 100 ps of its evolution before stabilising. Using short pulse pumping to produce a short pulse X-ray laser (pulse durations ~3 ps have been measured[16]) and a short pulse laser to heat the sample target will give improved uniformity and better temporal resolution of the opacity of the expanding plasma.

Acknowledgements

We acknowledge funding from the United Kingdom Engineering and Physical Sciences Research Council, the Council for the Central Laboratory of the Research Councils, the Ministry of Defence Joint Grants scheme and the Czech Science Foundation. We thank staff at the Central Laser Facility, Rutherford Appleton Laboratory for their assistance. We would also like to thank R. Keenan and A. MacPhee for their helpful contribution and discussions.

References

1. L. B. Da Silva *et al*., *Phys. Rev. Lett.* **69**, 438 (1992).
2. C. Chenais-Popovics *et al*., *Astrophys. J. Suppl.* **127**, 275 (2000)
3. J. M. Foster *et al*., *Phys. Rev. Lett.* **67** 3255-3258 (1991)
4. K. Nazir *et al*., *Appl. Phys. Lett.* **69**, 3686 (1996)
5. G. B. Rybicki and A. P. Lightman *Radiative processes in astrophysics* (Wiley: New York, 1979), p. 39
6. K. O'Nions, P. Pitman and C. Marsh, *Nature* **415**, 853 (2002)
7. S. V. Milton *et al*., *Science* **292**, 2037 (2001)
8. M. Fajardo, P. Zeitoun and J. C. Gauthier, *Eur. Phys. J. D*, **29**, 69 (2004)
9. G. J. Tallents *J. Phys D: Appl. Phys.* **36**, 259-276 (2003)
10. B.L. Henke, E.M. Gullikson, and J.C. Davis. *X-ray interactions: photo-absorption, scattering, transmission, and reflection at E=50-30000 eV, Z=1-92*, Atomic Data and Nuclear Data Tables Vol. 54 (no.2), 181-342 (July 1993)
11. N. H. Magee, Jr., J. Abdallah, Jr., R. E. H. Clark, *et al*., *Atomic Structure Calculations and New Los Alamos Astrophysical Opacities*, Astronomical Society of the Pacific Conference Series (Astrophysical Applications of Powerful New Databases, S. J. Adelman and W. L. Wiese eds.) **78**, 51 (1995)
12. *TOPS: A Multigroup Opacity Code*; Los Alamos Report LA-10454, by Joseph Abdallah, Jr. and Robert E. H. Clark
13. W. F. Huebner, A. L. Merts, N. H. Magee, Jr., M. F. Argo, *Astrophysical Opacity Library*; Los Alamos Report LA-6760-M
14. *The Los Alamos LEDCOP code*; Los Alamos Report LA-UR-97-1038, by N. H. Magee, A. L. Merts, J. J. Keady and D. P. Kilcrease
15. M. H. Edwards *et al*., *Phys. Rev. Lett.* **97**, 035001 (2006)
16. A. Klisnick *et al*., *Phys. Rev. A* **65** 033810 (2002)